

Numerical analysis of a free piston problem*

BORIS MUHA¹ AND ZVONIMIR TUTEK^{1,†}

¹ *Department of Mathematics, University of Zagreb, Bijenička 30, HR-10 000 Zagreb, Croatia*

Received October 28, 2009; accepted June 22, 2010

Abstract. The problem considered is the Stokes and Navier-Stokes flow through a system of two pipes in the gravity field; inside a vertical pipe there is a free heavy piston. Theoretical analysis, the existence and non-uniqueness of solution, has been completed recently by the authors. Here we present numerical analysis, using finite elements methods, of the stationary state with respect to the angle between the two pipes, diameters of the pipes, search for solution of a full problem and search for bifurcation points. The analysis is carried out for both, 2D and 3D, and for Stokes and Navier-Stokes case.

AMS subject classifications: 65N30, 65N99, 76D05

Key words: free piston problem, Navier-Stokes equations, numerical analysis

1. Introduction

1.1. Notation and geometry of the problem

We consider a flow of incompressible Newtonian heavy fluid in a system of two converging pipes. The system is constituted by a horizontal and a “vertical” pipe. The horizontal pipe \mathcal{F}_1 is infinite with a constant cross-section S_1 of diameter d_1 . Nevertheless, we consider only a control volume Ω_1 of length L which is large enough to let, in correspondence with constant pressure gradient, Poiseuille flow develop at the two exits, Σ_p and Σ_k , respectively. At the center of Ω_1 on a rigid lateral wall the second semi-infinite pipe \mathcal{F}_2 , with a constant cross-section of diameter d_2 , is connected. The axis of \mathcal{F}_2 is inclined to the vertical by an angle α . Inside the “vertical” pipe \mathcal{F}_2 we have a heavy piston, with cross-section of diameter d , which can translate freely along the “vertical” pipe \mathcal{F}_2 without rotations. A lower basis of the piston is horizontal (see Figure 1). Therefore, d and d_2 cannot be chosen arbitrary but some compatibility condition must be satisfied. In all numerical examples cross-sections S_1 and S_2 will be circular and then we have $d = d_2 / \cos \alpha$. Friction between the wall of \mathcal{F}_2 and the piston is neglected.

Fluid enters the “vertical” pipe \mathcal{F}_2 only up to equilibrium height of the piston. Let us call Ω_2 the region of the \mathcal{F}_2 filled with the fluid. Let Σ_h denote the upper horizontal boundary of Ω_2 . The piston is modeled as a rigid body. It is in equilibrium if and only if the total force is zero. Since the piston is a rigid body, fluid is at rest on

*Presented at the Sixth Conference on Applied Mathematics and Scientific Computing, Zadar, Croatia, September 2009.

†Corresponding author. *Email addresses:* borism@math.hr (B. Muha), tutek@math.hr (Z. Tutek)

Σ_h . Motion of the fluid is given by Navier-Stokes equations. We will consider both, a 2D and 3D case. The goal of this paper is to numerically determine stationary fluid flow and equilibrium position of the piston and analyse its dependence on geometry, i.e. on an angle α and a ratio $\frac{d_1}{d_2}$. Furthermore, we will analyse non-uniqueness of the stationary flow. The main realistic example will be blood flow through arterioles.

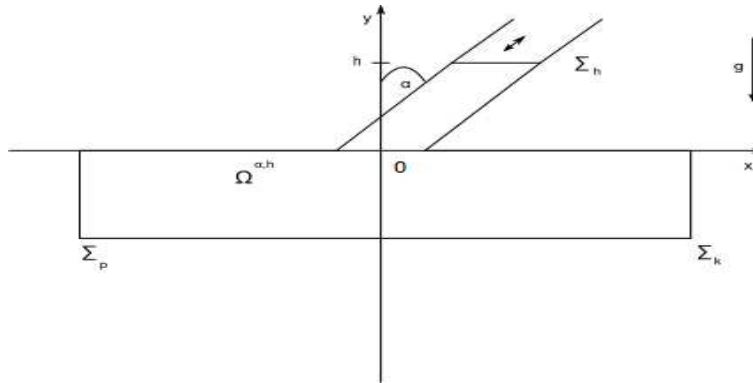


Figure 1. Ω_h^α

Let us now introduce some notations and precise assumption on the geometry. Coordinate \mathbf{x} (in 3D case $\mathbf{x} = (x_1, x_2)$ and in 2D case $\mathbf{x} = x_1$) is along the horizontal pipe and y is in the opposite direction of acceleration of gravity. Let h be the height of the piston in the selected coordinate frame, $\Omega_h^\alpha \subset \mathbb{R}^n$, $n = 2, 3$ the domain occupied by the fluid. More precisely, $\Omega_h^\alpha = \Omega_1 \cup \Omega_0 \cup \Omega_2^{h,\alpha}$, where

$$\Omega_1 = \{(x_1, x_2, y); -L \leq x_1 \leq L, (x_2, y) \in S_1\}, \quad S_1 \subset \mathbb{R}^2.$$

Let $\mathbf{s} = \cos \alpha \mathbf{e}_{x_1} + \sin \alpha \mathbf{e}_y$ be the direction of the “vertical” pipe \mathcal{F}_2 . Then in the non-orthogonal coordinate frame $(\mathbf{e}_{x_1}, \mathbf{e}_{x_2}, \mathbf{s})$, $\Omega_2^{h,\alpha}$ has the form:

$$\Omega_2^{h,\alpha} = \{(z_1, z_2, z_3); 0 \leq z_3 \leq h/\cos \alpha, (z_1, z_2) \in \Sigma\}, \quad \Sigma \subset \mathbb{R}^2.$$

Only $\Omega_2^{h,\alpha}$ depends on h and α . The lower basis of the piston Σ_h will be considered as a subset of the $y = \text{const}$ plane. The origin of the coordinate frame is chosen in a such way that the lower end of the “vertical” pipe Σ_0 is a subset of $y = 0$ plane. We assume that Σ_0 is a symmetric w.r.t. plane perpendicular to the central axis of the horizontal pipe. Furthermore, we suppose that $\Omega_0 \cup \Omega_1$ (a domain without the “vertical” pipe) is also a symmetric w.r.t. plane perpendicular to the central axis of the horizontal pipe; this is a technical assumption and not a restriction. Note that Ω_0 is an extension of the vertical pipe up to the boundary of Ω_1 ; its shape is complicated in general in a 3D case, in a 2D case it is empty set. Inflow and outflow regions are denoted by Σ_p and Σ_k , respectively. $\Gamma = \partial\Omega_h^\alpha \setminus (\Sigma_p \cup \Sigma_k \cup \Sigma_h)$ is a rigid boundary. We suppose that the domain is locally Lipschitz. This is a natural assumption because one cannot expect a smoother domain because we will always have an angle at the contact of the piston and rigid boundary.

1.2. Formulation of the problem

Since the fluid is modeled by the Navier-Stokes equations, the stress tensor is given by $T = -pI + 2\mu \text{sym}(\nabla \mathbf{u})$, where \mathbf{u} is velocity of the fluid, p pressure and μ viscosity. Total fluid force on the piston in direction \mathbf{s} is given by formula:

$$F^\alpha(h) = - \int_{\Sigma_h} T \mathbf{n} \cdot \mathbf{s}, \tag{1}$$

where \mathbf{n} denotes the unit outer normal; here $\mathbf{n} = \mathbf{e}_y$. For simplicity, we will omit index α in the unknowns. Differential formulation of our problem is:
 find $(\mathbf{u}, p, h) \in H^1(\Omega_h^\alpha)^3 \times L^2(\Omega_h^\alpha) \times \mathbb{R}_+$ such that

$$\begin{aligned} -\mu \Delta \mathbf{u} + \varrho(\nabla \mathbf{u})\mathbf{u} + \nabla p &= -g\varrho \mathbf{e}_y & \text{in } \Omega_h^\alpha, \\ \text{div } \mathbf{u} &= 0 & \text{in } \Omega_h^\alpha, \\ \mathbf{u} &= 0 & \text{on } \Gamma, \\ \mathbf{u} &= 0 & \text{on } \Sigma_h, \\ \mathbf{u} \times \mathbf{n} = 0, p &= P_{p/k} - g\varrho y & \text{on } \Sigma_{p/k}, \\ F^\alpha(h) &= P_0. \end{aligned} \tag{2}$$

Here ϱ is the density of the fluid, μ dynamic viscosity, g gravity constant and P_0 constant that takes into account the weight of the piston and atmospheric pressure. The angle α is given. The first two equations are just the Navier-Stokes equations for stationary flow of an incompressible Newtonian fluid. Boundary conditions $(2)_3$ and $(2)_4$ are no slip boundary conditions on rigid boundary. Condition $(2)_6$ is a balance of forces on the piston. $F^\alpha(h)$ is well defined because with our choice of function spaces we have $T \in L^2(\Omega_h^\alpha)^{3 \times 3}$ and $\text{div } T \in L^{\frac{3}{2}}(\Omega_h^\alpha)^3$. P_p and P_k are constants and since flow is driven by the difference of pressures on inflow and outflow boundary, we can assume that $P_p = -P_k$ (with a possible redefinition of constant P_0). Fixing the pressure does not affect total force on the piston since relevant quantity is the difference between the atmospheric pressure and fluid pressure. Term $-g\varrho y$ in $(2)_5$ comes from the hydrostatic pressure. These types of non-standard boundary conditions involving pressure were studied in [1] and [3]. The problem has two non-linearities. One that comes from the Navier-Stokes equations is classical (see [6]). The second comes from the fact that the domain is unknown and therefore F^α is a nonlinear function. We will also consider Stokes case where the fluid is modeled with the Stokes equations.

We will often refer to the Stokes or Navier-Stokes problem in a fixed domain, more precisely for $h \in \mathbb{R}_+$ fixed, find $(\mathbf{u}, p) \in H^1(\Omega_h^\alpha)^3 \times L^2(\Omega_h^\alpha)$ such that $(2)_{1-5}$ holds. This problem will be denoted by (S_h) , (NS_h) for Stokes and Navier-Stokes case, respectively.

2. Overview of theoretical results

In this chapter we will briefly summarize theoretical results; details can be found in [4]. Since domain Ω_h^α is only locally Lipschitz and has concave points, solution

(\mathbf{u}_h, p_h) of Navier-Stokes system (NS_h) has only $H^1 \times L^2$ regularity. However, by using techniques from [3] it can be proven that formula (1) can be understood in an $H^{-1/2}(\Sigma_h)$ sense.

Lemma 1. *Let (\mathbf{u}_h, p_h) be the solution of Stokes (S_h) or Navier-Stokes (NS_h) system in Ω_h^α . Then for every $h \geq 0$ we have*

$$F^\alpha(h) = \cos \alpha \int_{\Sigma_h} p_h - \mu \sin \alpha \int_{\Sigma_h} \partial_y (\mathbf{u}_h)_{x_1},$$

where the integral is taken in an $H^{-1/2}(\Sigma_h)$ sense.

Furthermore, we have an existence result.

Theorem 1. *In the Stokes case, there exists $P \in \mathbb{R}$ such that for every $P_0 \leq P$ problem (2) has at least one solution $(\mathbf{u}_h, p_h, h) \in H^1(\Omega_h) \times L^2(\Omega_h) \times \mathbb{R}_+$. In the Navier-Stokes case we have the same conclusion provided that data $|P_p|$ and $|P_k|$ are small enough.*

In general, even in the Stokes case we do not have a uniqueness result and bifurcation phenomena can occur. More precisely, we have the following result:

Theorem 2. *There exist α and P_0 with corresponding stationary state (\mathbf{u}_0, p_0, h_0) in which we have a turning point. More precisely, (\mathbf{u}_0, p_0, h_0) is a solution of the Stokes case of problem (2) and all solutions of this problem in some neighborhood of (\mathbf{u}_0, p_0, h_0) belong to some curve $(X(s), P(s))$ with $X(0) = (\mathbf{u}_0, p_0, h_0)$ and $P(0) = P_0$. Furthermore, tangent at $(X(0), P(0))$ is $(V, 0)$ and P does not have a saddle point at 0.*

In the next chapter we will give a numerical illustration of this theorem. Numerical results suggest uniqueness of the bifurcation point. One of the goals of this paper is a numerical search for the bifurcation point and analysis of its dependence on geometry. In order to do that, we will need some additional theoretical results about function F . As a corollary in proof of the Theorem 2 we concluded that function F defined in (1) belongs to $C^1(\mathbb{R}_+)$. Furthermore, we can get an expression for its derivative with respect to h :

$$(F^\alpha)'(h) = \cos \alpha \int_{\Sigma_h} P - \mu \sin \alpha \int_{\Sigma_h} \left(\partial_y U_{x_1} - \frac{1}{h} \partial_y (\mathbf{u}_0)_{x_1} \right).$$

Here P is a solution of the problem:

find $(\mathbf{U}, P) \in \mathcal{V} \times L^2(\Omega_h^\alpha)$ such that

$$\begin{aligned} \int_{\Omega_h^\alpha} \nabla \mathbf{U} \cdot \nabla \mathbf{v} - \int_{\Omega_h^\alpha} P \nabla \cdot \mathbf{v} &= -\frac{1}{h} \int_{\Omega_2^{h,\alpha}} \left(\nabla \mathbf{u}_0 \cdot \nabla \mathbf{v} - p_0 \nabla \cdot \mathbf{v} \right. \\ &\quad - \begin{pmatrix} \mathbf{0} \\ \tan(\alpha) \partial_x + \partial_y \end{pmatrix} \mathbf{u}_0 \cdot \nabla \mathbf{v} \\ &\quad - \frac{1}{h_0} \nabla \mathbf{u}_0 \cdot \begin{pmatrix} \mathbf{0} \\ \tan(\alpha) \partial_x + \partial_y \end{pmatrix} \mathbf{v} \\ &\quad \left. - p_0 \nabla \cdot \mathbf{v} + p_0 \begin{pmatrix} \mathbf{0} \\ \tan(\alpha) \partial_x + \partial_y \end{pmatrix} \cdot \mathbf{v} \right), \quad \mathbf{v} \in \mathcal{V}, \\ \int_{\Omega_h^\alpha} q \nabla \cdot \mathbf{U} &= -\frac{1}{h} \int_{\Omega_2^h} (\tan \alpha \partial_x (\mathbf{u}_0)_y + \partial_y (\mathbf{u}_0)_y), \quad q \in L^2(\Omega_h^\alpha), \end{aligned} \tag{3}$$

where (\mathbf{u}_0, p_0) is a solution of Stokes system (S_h) in Ω_h^α and

$$\mathcal{V} = \{ \mathbf{v} \in H^1(\Omega_h^\alpha)^3; \mathbf{v} = 0 \text{ on } \Gamma \cup \Sigma_h, \mathbf{v} \times \mathbf{n} = 0 \text{ on } \Sigma_{p/k} \}.$$

We will use this formula later in Example 4.

3. Numerical experiments

In this section we will present numerical experiments that provide better understanding of the problem. All experiments in a 2D case are done using FreeFem++ 3.4. and visualization is made by Mathematica 5.2. Triangulation and visualization of solutions in a 3D case are made using Gmsh, while matrix assembly and solving of linear systems are done in FreeFem.

In both, a 2D and a 3D case, continuous piecewise quadratic and continuous piecewise linear elements for velocity and pressure, respectively, are used. Mesh size is indicated by density of arrows in velocity field figures.

Before stating results of numerical experiments we want to emphasize one simple fact. Let $p_H(\mathbf{x}, y) = -\rho g y$ be the hydrostatic pressure. Then all solutions of system (NS_h) have form $(\mathbf{u}_h, q_h + p_H)$, where (\mathbf{u}_h, q_h) is a solution of homogenous system (NS_h) ($g = 0$). In the sequel we will present results for (\mathbf{u}_h, q_h) since hydrostatic pressure can be added easily.

3.1. Stokes case

When we consider Stokes case, we can, without loss of generality, assume $\mu = 1$ because if (\mathbf{u}, p) is a solution of problem (S_h) for $\mu = 1$ then $(\mathbf{u}/\mu, p)$ is a solution of problem (S_h) for general μ .

3.1.1. 2D case

In the next few examples we will analyse dependence of function $F^\alpha(h)$ on α . Geometrical parameters are $L = 10$, $P_{p/k} = \pm 5$, $d_1 = 1.6$, $d = 1.6$ and we vary α and h .

Example 1. *This example illustrates asymptotic behaviour of function F^α . We take $\alpha = \frac{\pi}{3}$ fixed and vary height h from 0 to 16 with step 0.08. For every h we solve problem $(S_h^{\frac{\pi}{3}})$ in $\Omega_h^{\frac{\pi}{3}}$ and compute $F^{\frac{\pi}{3}}(h)$. We keep the maximal diameter of a triangle in triangulation approximately the same.*

In Figure 2 we can see that function $F^{\frac{\pi}{3}}$ approaches its asymptotic value very fast.

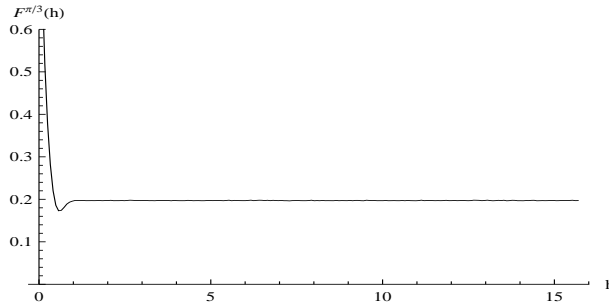


Figure 2. Graph of function $F^{\frac{\pi}{3}}$

Example 2. *The second example shows a graph of function F^α . For every h , Stokes system (S_h^α) in Ω_h^α is solved and $F^\alpha(h)$ computed. Notice that in this example we solve a series of Stokes problems (S_h) in fixed domains and we do not solve full original problem (2).*

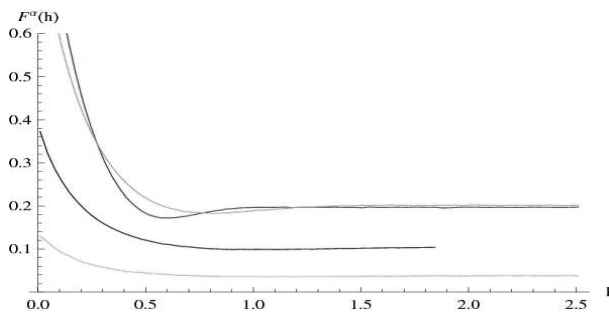


Figure 3. Graphs of functions $F^{1.05}$, $F^{0.79}$, $F^{0.31}$ and $F^{0.11}$

In Figure 3 graphs of $F^{1.05}$ (red), $F^{0.79}$ (green), $F^{0.31}$ (blue) and $F^{0.11}$ (violet) are given. One can notice that for all α , F^α have the same qualitative behaviour, i.e. first, it is strictly monotone on some interval and then it has a critical point after which it asymptotically approaches some constant at infinity. Asymptotic decay can be proved using Leray's flow (see [4]). This example is a good illustration of Theorem 2 because we can see that F attains the same value for different height h . Since for every h we can find related (\mathbf{u}_h, p_h) , we have two stationary states for some P_0 .

Example 3. *With this example we will illustrate non-uniqueness of a solution of problem (2) more precisely. We will show two different flows which act upon the*

piston with the same force. We take $\alpha = \frac{\pi}{3}$ and solve problem (S_h) for $h_1 = 0.465$ and $h_2 = 0.98$. Then we compute $F^{\frac{\pi}{3}}(0.465) = 0.19637$ and $F^{\frac{\pi}{3}}(0.98) = 0.196608$. Furthermore, we compute total fluid force on the piston in point $h_3 = 0.6$, $F^{\frac{\pi}{3}}(0.6) = 0.173024$.

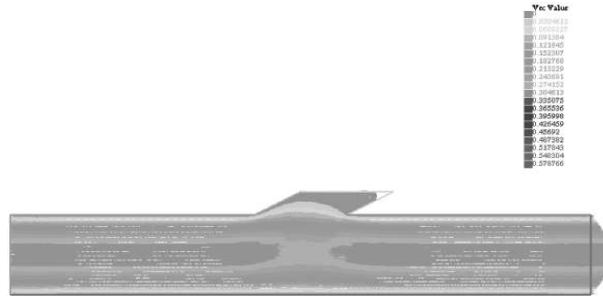


Figure 4. Velocity field in domain $\Omega_{0.46}^{\frac{\pi}{3}}$

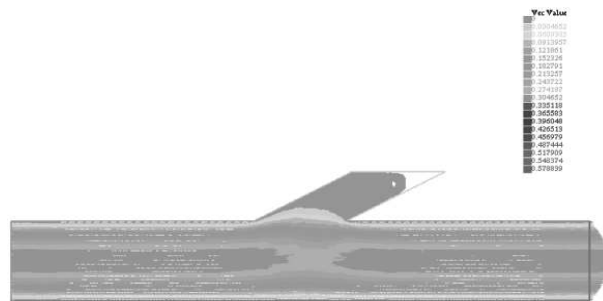


Figure 5. Velocity field in domain $\Omega_{0.98}^{\frac{\pi}{3}}$

Example 4. We take fixed outer pressure $P_V = 0.3125$ and solve full problem (2) using Newton's method. More precisely, we use Newton's method for solving equations $F^\alpha(h) = P_0(\alpha, d)$, where $P_0(\alpha, d) = P_V \cos \alpha * d$. We will vary parameters of geometry (α and d) and consider dependence of equilibrium height of the piston on geometry.

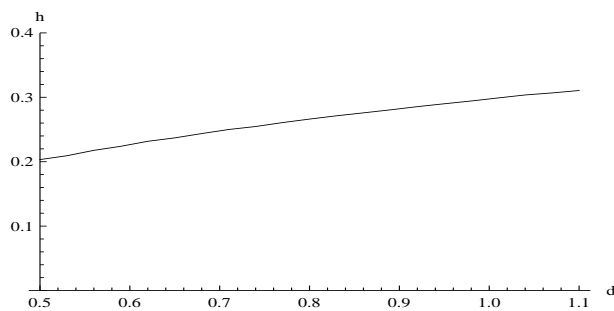


Figure 6. Dependence of equilibrium height on diameter of the piston d

Figures 6 and 7 show dependence of equilibrium height h of the piston on diameter of the piston d and angle α , respectively. One can see that height h is greater for greater d and greater α . The solution is in general not unique, so a numerical solution depends on initial guess in Newton's method. In this example we took initial

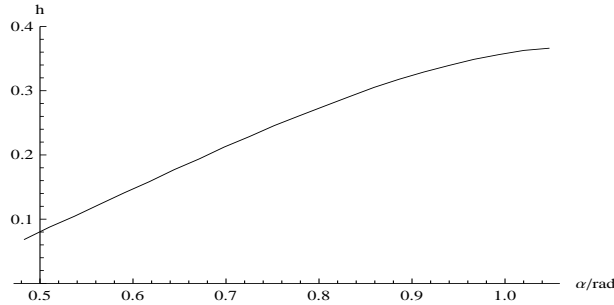


Figure 7. Dependence of equilibrium height on angle α

guess on interval where F is decreasing. If we took initial guess on height where F stabilizes and $g \neq 0$, equilibrium height would depend only on the asymptotic value of pressure as $h \rightarrow \infty$. Namely, we know that F^α asymptotically approaches to some constant $\cos \alpha C_\alpha$ (see [4] and Figure 2) and therefore a balance of forces is approximately reduced to $\cos \alpha C_\alpha - \rho gh = P_0(\alpha)$ for h great enough. In the next example we will analyse constant C_α more closely.

Example 5. As we have proven in [4], for every given geometry and data there exists constant C_α such that $\lim_{h \rightarrow \infty} F^\alpha(h) = \cos \alpha C_\alpha$. The goal of this example is to analyse dependence of constants C_α on parameter α . We take all parameters the same as in the previous example, $h = 3$ (which is large enough) and vary parameter α between 0 and $\frac{1}{3}\pi$ with step $\frac{\pi}{120}$ and compute $F^\alpha(3)$. Since it is easy to verify symmetry property $F^{-\alpha}(h) = -F^\alpha(h)$, we do not need to compute negative α -s. Again, we emphasize that here we do not solve full problem (2), but problem (S_h) for some fixed parameters in order to provide better understanding of qualitative behaviour of total force F^α .

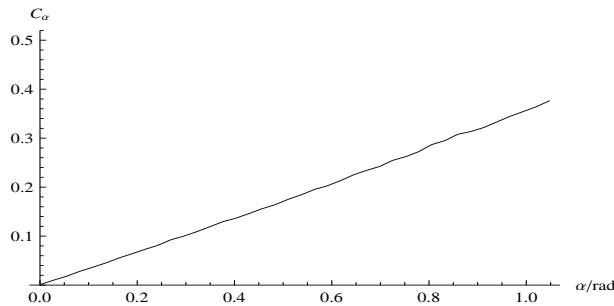


Figure 8. Dependence of constant C_α on angle α

Figure 8 strongly suggests linear dependence of asymptotic force on angle α .

Example 6. We compute bifurcation point h_B for various α by solving equation $(F^\alpha)'(h) = 0$. The bisection method is used because computation of $(F^\alpha)''$ is too expensive and would result in an additional numerical error. This time we take $\alpha < 0$. We can directly compute results for $\alpha > 0$ using symmetry property $F^{-\alpha}(h) = -F^\alpha(h)$.

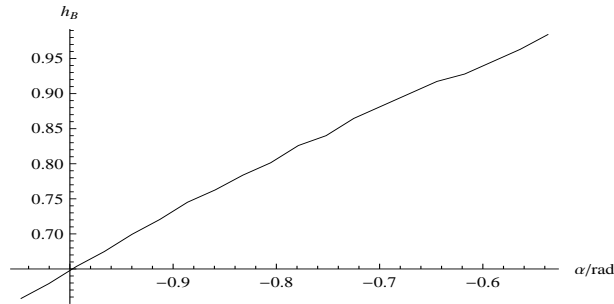


Figure 9. Dependence of bifurcation point h_B on angle α

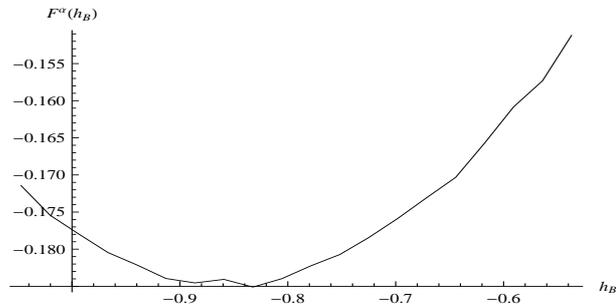


Figure 10. Value of function F^α in bifurcation point

Figure 9 shows that the bifurcation point will be reached earlier for α closer to 0. This is in accordance with Figure 3 and related discussion afterwards. Figure 10 has a physical interpretation of maximal total outer force in direction \mathbf{s} on the piston that the flow can support.

3.1.2. 3D case

In a 3D, case numerical experiments suggest similar behaviour of solutions as in a 2D case, but of course computations are more complex and therefore we cannot use triangulations fine enough to ensure a numerical error to be as low as in a 2D case. Here we present an example illustrating it.

Example 7. Geometrical parameters are $L = 10$, $P_{p/k} = \pm 5$, $d_1 = 3$, $d = 2$.

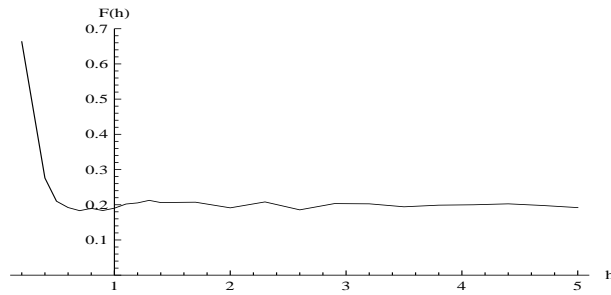
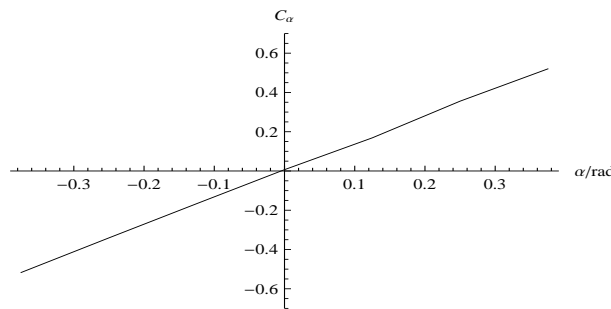
Figure 11. Graph of function $F^{\frac{\pi}{3}}$ Figure 12. Dependence of C_α on angle α

Figure 11 shows analogous behaviour of function F^α as in a $2D$ case. As we have explained before, small variations after the bifurcation point are due to a numerical error. Figure 12 suggests that linear dependence of constant C_α on α is not a property of a $2D$ case, but it also holds in a $3D$ case.

3.2. Navier-Stokes case

For every fixed h , we will solve the Navier-Stokes problem (NS_h) using Newton's method described in [2]. In every step of Newton's method we will solve the linearized Navier-Stokes system. We will use a solution of the Stokes system for initial guess in Newton's iterations. Therefore, in this section we will only consider laminar flow for which we also have theoretical results (see Section 2). In the Navier-Stokes case we will lose symmetry properties that we had in the Stokes case and we will illustrate those differences with the following few numerical examples.

Example 8. *We will consider blood flow through larger arterioles. Since in this case vessel diameter is much larger than cell diameters, we can assume that blood has constant viscosity $\mu = 0.003 \text{ Pa}\cdot\text{s}$ and it is Newtonian (see [5]). Other data are: density $\rho = 1060 \frac{\text{kg}}{\text{m}^3}$, diameters of vessels $d_1 = 0.05\text{mm}$, $d = 0.03\text{mm}$, length $L = 0.4\text{mm}$ (part of this length is enough to show effects near the junction) and pressure drop $\delta p = 125 \frac{\text{Pa}}{\text{m}}$. Reynolds number of this flow is 0.07 . Furthermore, we will consider the same flow in a $2D$ case and make analysis of dependence of total force on the angle and height.*

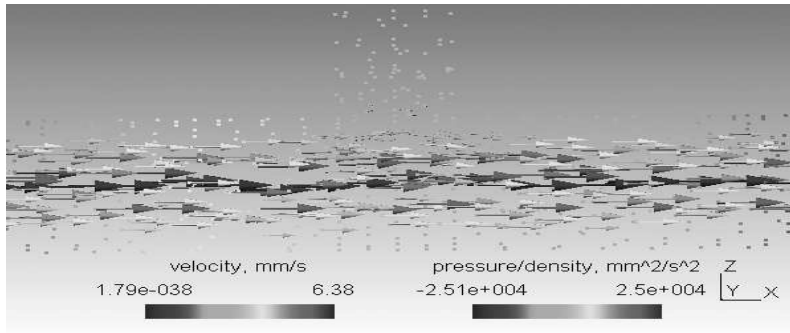


Figure 13. *Solution (\mathbf{u}, p) in Ω^0*

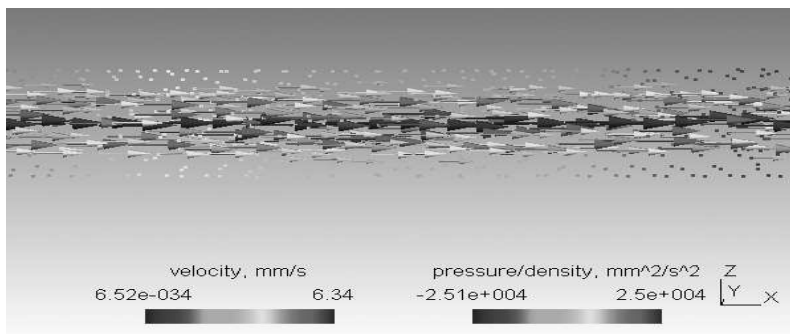


Figure 14. *Solution (\mathbf{u}, p) in Ω_1*

Figures 13 and 14 (here $\mathbf{x} = (x, y)$, $y = z$) show solution (\mathbf{u}, p) of problem (NS_h) in Ω^0 (case when pipes are perpendicular) and Ω_1 (just horizontal pipe), respectively. One can see that we have taken a segment of arteriola that is long enough to allow a fully developed Poiseuille flow in the horizontal pipe. The only significant difference between flows in Figures 13 and 14 is near the junction of the pipes and therefore only this part is plotted.

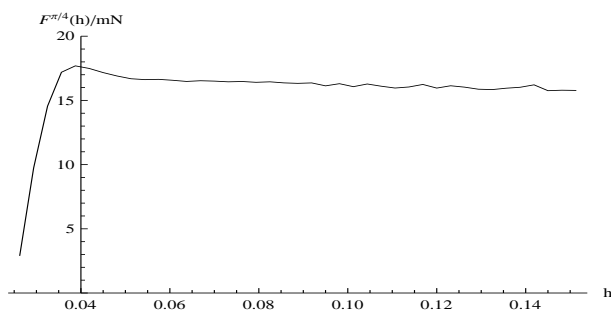


Figure 15. *Graph of function $F^{\frac{\pi}{4}}$*

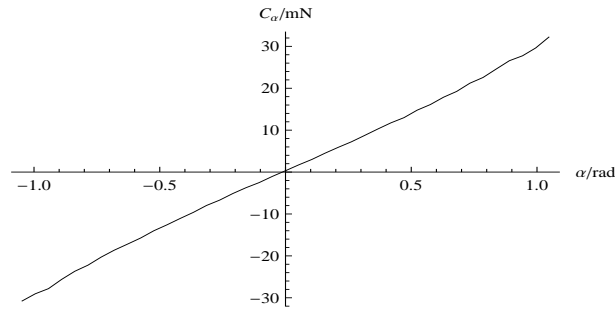


Figure 16. Dependence of total force C_α on angle α

Figure 15 shows that the function of total force F^α has the different qualitative, but same asymptotic behaviour as in Stokes case. From Lemma 1 we see that x_1 component of force F^α is negligible due to the smallness of parameter μ ($\mu = 3 \cdot 10^{-6} \text{ kg/mms}$). However, due to the fact that the flow is still laminar, we have only a negligible non-linear effect from the fluid and behaviour of the total fluid pressure on the piston stays the same as in the Stokes case.

Finally, Figure 16 shows that linear dependence of total force on α was a linear effect and in Navier-Stokes case we do not have this effect anymore even in the case of a laminar flow. One can notice that blood flow through arterioles has a very low Reynolds number (around 0.07) and therefore non-linear effects are not so pronounced. If we take a more turbulent flow (Reynolds number around 800), yet still laminar (Figure 17), we can notice that dependence of force on angle α has different qualitative behaviour. However, qualitative behaviour of F^α in dependence of h stays the same as in the case of the Stokes flow and the blood the flow (Figure 15) because flow is still laminar.

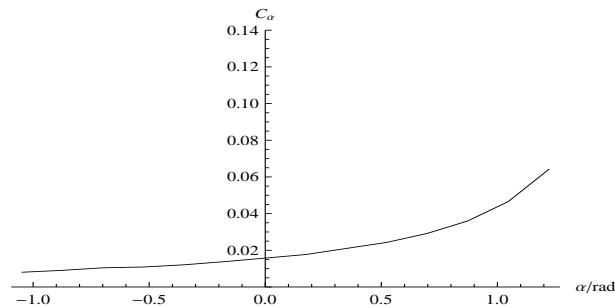


Figure 17. Dependence constant C_α on angle α

References

- [1] C. CONCA, F. MURAT, O. PIRONNEAU, *The Stokes and Navier-Stokes equations with boundary conditions involving the pressure*, Japan J. Math **20**(1994), 297–318.
- [2] V. GIRAULT, P. A. RAVIART, *Finite Elements Methods for Navier-Stokes Equations, Theory and Algorithms*, Springer-Verlag, Berlin, 1986.

- [3] E. MARUŠIĆ-PALOKA, *Rigorous justification of the Kirchhoff law for junction of thin pipes filled with viscous fluid*, *Asymptot. Anal.* **33**(2003), 51–66.
- [4] B. MUHA, Z. TUTEK, *On a free piston problem for Stokes and Navier-Stokes equations*, submitted, available at [http://web.math.hr/~\thicksim\\$borism/preprints/free_piston.ps](http://web.math.hr/~\thicksim$borism/preprints/free_piston.ps).
- [5] J. T. OTTESEN, M. S. OLUFSEN, J. K. LARSEN, *Applied Mathematical Models in Human Physiology*, SIAM Monographs on Mathematical Modeling and Computation, Philadelphia, 2004.
- [6] R. TEMAM, *Navier-Stokes equations: theory and numerical analysis*, AMS Chelsea Publishing, Providence, 2000.